



# Angio-associated migratory cell protein interacts with epidermal growth factor receptor and enhances proliferation and drug resistance in human non-small cell lung cancer cells



Shun Yao<sup>a</sup>, Feifei Shi<sup>a</sup>, Yingying Wang<sup>a,b</sup>, Xiaoyang Sun<sup>a</sup>, Wenbo Sun<sup>a</sup>, Yifeng Zhang<sup>a</sup>, Xianfang Liu<sup>c</sup>, Xiangguo Liu<sup>a,b,\*</sup>, Ling Su<sup>a,b,\*</sup>

<sup>a</sup>Shandong Provincial Key Laboratory of Animal Cell and Developmental Biology, School of Life Sciences, Shandong University, Qingdao, China

<sup>b</sup>Shandong Provincial Collaborative Innovation Center of Cell Biology, School of Life Sciences, Shandong Normal University, Jinan, China

<sup>c</sup>The Department of Otolaryngology Head and Neck Surgery, Shandong Provincial Hospital, Affiliated to Shandong University, Jinan, China

## ARTICLE INFO

### Keywords:

AAMP  
Proliferation  
Tumorigenesis  
EGFR  
Icotinib  
Doxorubicin

## ABSTRACT

Angio-associated migratory cell protein (AAMP) is expressed in some human cancer cells. Previous studies have shown AAMP high expression predicted poor prognosis. But its biological role in non-small cell lung cancer (NSCLC) cells is still unknown. In our present study, we attempted to explore the functions of AAMP in NSCLC cells. According to our findings, AAMP knockdown inhibited lung cancer cell proliferation and inhibited lung cancer cell tumorigenesis in the mouse xenograft model. Epidermal growth factor receptor (EGFR) is a primary receptor tyrosine kinase (RTK) that promotes proliferation and plays an important role in cancer pathology. We found AAMP interacted with EGFR and enhanced its dimerization and phosphorylation at tyrosine 1173 which activated ERK1/2 in NSCLC cells. In addition, we showed AAMP conferred the lung cancer cells resistance to chemotherapeutic agents such as icotinib and doxorubicin. Taken together, our data indicate that loss of AAMP from NSCLC inhibits tumor growth and elevates drug sensitivity, and these findings have clinical implications to treat NSCLC cancers.

## 1. Introduction

Angio-associated migratory cell protein (AAMP) was initially isolated from a human melanoma cell line in 1995 [1]. AAMP is a 52kD protein that contains two immunoglobulin-like domains, a heparin binding consensus sequence and a repeat WD40 motif which plays various roles in cell cycle control, protein-protein interaction, transcriptional activation, and signal transduction [2,3]. AAMP is expressed in different cell types, including smooth muscle cells, dermal fibroblasts, renal proximal tubular cells and cancerous cells like human breast carcinoma cells, melanoma cells and prostate cancer cells [4–8].

Recent studies suggest AAMP plays an important role in angiogenesis by promoting endothelial tube formation [9,10]. And, it is implicated in cell migration via the ROCK/RHOA signaling pathway [11]. AAMP was also reported to affect cell growth in HECV cells, but its

mechanism is still unknown [12]. AAMP expression is increased in a number of cancer cells like invasive gastrointestinal and breast carcinoma cells; it is considered a marker of poor prognosis [13,14].

The epidermal growth factor receptor (EGFR), which is anchored in the cytoplasmic membrane, belongs to the ERBB family of receptor tyrosine kinases [15]. EGFR is widely expressed and plays a critical role in cell growth, proliferation and differentiation [16]. Dimerization is essential for EGFR activation in healthy cells. When activated, the COOH-terminal portion is phosphorylated at specific sites, such as 1173 tyrosine, which initiates intracellular signaling pathways [15,17]. As expected, dysregulated EGFR activation is found in multiple cancer cells, including lung cancer, indolent bronchioalveolar carcinoma and non-small cell lung cancer [18,19].

Overexpression and mutations are the main causes of EGFR dysregulation. Its overexpression causes positive signal activated

**Abbreviations:** NSCLC, non-small cell lung cancer cell; AAMP, Angio-associated migratory cell protein; EGFR, epidermal growth factor receptor; ERK1/2, extracellular regulated protein kinase; RTK, receptor tyrosine kinase; CCND, Cyclin-D; ACTB,  $\beta$ -actin; EGF, epidermal growth factor; SRB, sulforhodamine B; CTTM, cytoplasmic and transmembrane fragment of EGFR; ETTM, cellular and transmembrane fragment of EGFR; CT, cytoplasmic fragment of EGFR; CASP3, caspase3; CASP8, caspase8

\* Corresponding authors at: Shandong University School of Life Sciences, Room N8-110, 72 Binhai Road, Qingdao 266237, China.

E-mail addresses: [xgliu@sdu.edu.cn](mailto:xgliu@sdu.edu.cn) (X. Liu), [suling@sdu.edu.cn](mailto:suling@sdu.edu.cn) (L. Su).

<https://doi.org/10.1016/j.cellsig.2019.05.004>

Received 30 January 2019; Received in revised form 25 April 2019; Accepted 4 May 2019

Available online 07 May 2019

0898-6568/ © 2019 Elsevier Inc. All rights reserved.

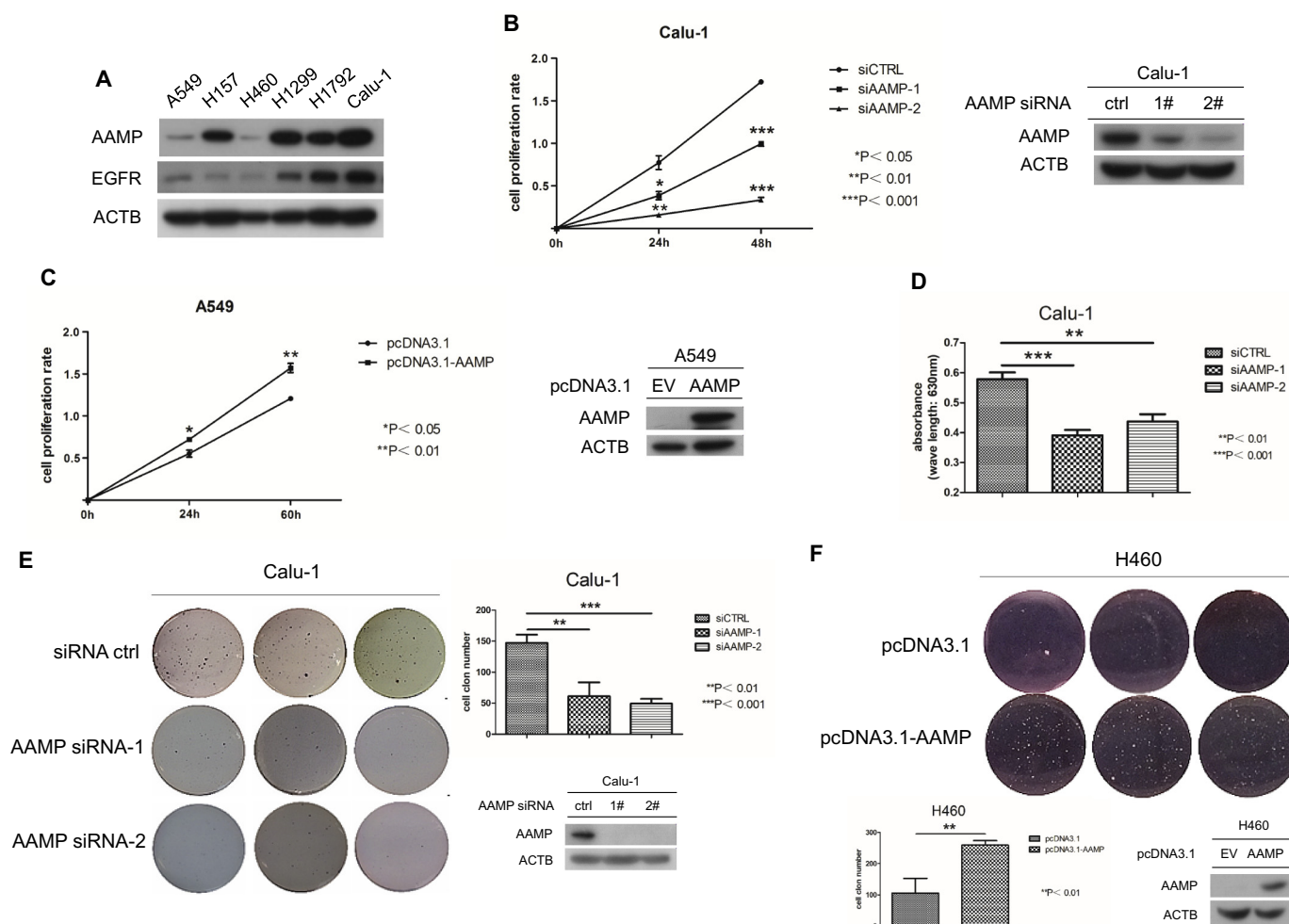


**Fig. 1.** AAMP inhibition impaired cell proliferation in NSCLC cells. (A) Western blot of AAMP from six non-small cell lung cancer cells. (B) Calu-1 cells were treated with AAMP siRNAs for 24 h and then reseeded in 24-well plates. Cells were imaged at 24 h and 48 h with high connotation microscope. Cell number and proliferation rate were calculated using provided software. The error bars represent the SD ( $n = 4$ ),  $*P < .05$ ,  $**P < .01$  and  $***P < .001$ . (C) AAMP was overexpressed in A549 cells for 24 h. Cells were reseeded in 24-well plates and imaged at 24 h and 60 h with high connotation microscope. Cell number and proliferation rate were calculated using software. The error bars represent the SD ( $n = 4$ ),  $*P < .05$  and  $**P < .01$ . (D) AAMP was silenced in Calu-1 cells for 24 h then cultivated in 96-well plates. EdU assay was performed according to instructions. The error bars represent the SD ( $n = 5$ ),  $***P < .001$ . (E) Calu-1 was transfected with AAMP siRNAs and then cultivated in agar culture medium for 24 h. Cells were stained after 7 days and cell number was calculated by software. The error bars represent the SD ( $n = 3$ ),  $**P < .01$  and  $***P < .0001$ . (F) Plasmid pcDNA3.1-AAMP and its empty control were transfected into H460 cells for 24 h. Cells were re-cultivated in agar culture medium for 7 days and cell number was calculated by software. The error bars represent the SD ( $n = 3$ ),  $**P < .01$ .

continuously, resulting in proliferation out of control and drug resistance. In some cases, EGFR silencing sensitized tumor cells to doxorubicin-induced apoptosis [20]. Besides, EGFR activating mutations, including exon 19 detection an exon 21-point mutations, give the ability to escape negative regulation [21]. Because of the importance of EGFR, drugs targeted to mutational EGFR, such as gefitinib, erlotinib and icotinib, have been used for the treatment of lung cancers [19]. However, acquired resistance to these drugs was developed in long-term treatment. The specific mechanism of first-generation EGFR-TKIs resistance (e.g. gefitinib, erlotinib and icotinib) was a secondary T790M mutation acquisition [22]. The threonine to methionine mutation increases the affinity between ATP and EGFR in tyrosine kinase domain, thus repressing the binding of EGFR-TKIs to EGFR. The acquired resistance limits TKIs' long-term efficacy. Thus, it is significant to pursue strategies to overcome TKIs-resistance in NSCLC cells.

It has been predicted by affinity capture MS that AAMP interacts with EGFR [23], but the significance of this combination is still unknown. In this study, we show AAMP interact with EGFR and active MAPK signal pathway by promoting EGFR dimerization, which enhanced tumor cell proliferation and tumorigenesis. In addition, we also

find AAMP silencing enhances apoptosis caused by icotinib and doxorubicin in EGFR mutation and wide-type NSCLC cells.

## 2. Materials and methods

### 2.1. Cell culture

Human NSCLC cell lines were originally obtained from American Type Culture Collection. A549 and H1792 cell lines have been authenticated in Microread Gene Technology by STR analysis. H1792, Calu-1, H460, H1975 and A549 cell lines were maintained in RPMI1640 (Sigma Aldrich, R6504) supplemented with 10% (v/v) fetal bovine serum (FBS, Gibco).

### 2.2. Antibodies

Commercially available primary antibodies for the following proteins were used: AAMP (Invitrogen, #PA5-31454, 1:5000); EGFR (Santa Cruz, #sc-03, 1:3000); p-EGFR-Y1173 (Invitrogen, #MA5-15158, 1:8000); ERK1/2 (CST, #9102, 1:2000); p-ERK1/2 (CST, #4370P,

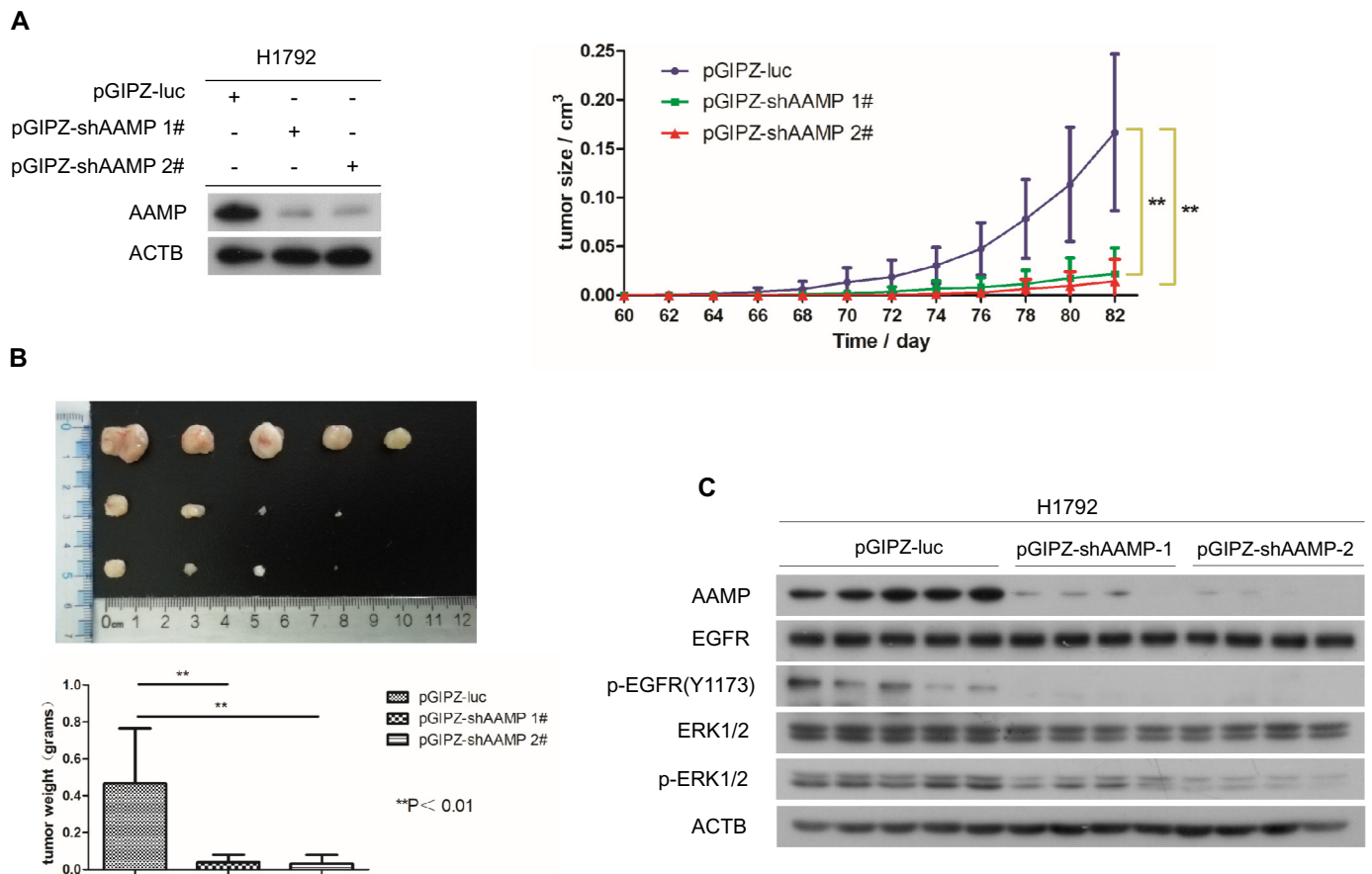


**Fig. 2.** Downregulation of AAMP suppressed H1792 xenograft growth *in vivo*. (A) B-NSG mice were injected with control cells or stably AAMP-silenced cells as indicated. The tumor size was measured every two days. Images show variation of tumor size after 60 days. The error bars represent the SD (n = 5), \*\*P < .01. WB showed AAMP expression in pGIPZ-luc and pGIPZ-shAAMP transfected H1792 cells. (B) The mice were sacrificed on the 82nd day. Tumors were dissected and weights were calculated. The error bars represent the SD, \*\*P < .01. (C) Tumors were dissected from mice and WB detected the level of phospho-EGFR (Y1173), phospho-ERK and AAMP in different group.

1:3000); CCND1 (CST, #2926, 1:2000); CCND3 (CST, #2936, 1:2000); CASP8 (CST, #1C12, 1:1000); CASP3 (NOVUS, #NB100-56708, 1:500); HA (Sangon Biotech, #AB10004, 1:10000); FLAG (Sigma-Aldrich, #F7425-2MG, 1:10000); ACTB (Sigma-Aldrich, #A1978, 1:10000).

### 2.3. siRNA and shRNA design

siAAMP-1 and siAAMP-2 siRNAs targeted the sequence 5'-GAGAG CTGTG GTAGGCTAT-3' and 5'-CUCUUAGGCAUCAGUGUCA-3', respectively. The lentiviruses containing AAMP 1st and 2nd shRNA were generous gifts from Shanghai Jiao Tong University College of Basic Medical Sciences, Shanghai, China.

### 2.4. Plasmids

The AAMP ORF sequence was amplified from Calu-1 cDNA using the following primers: sense, 5'-GGG TACCGCCGCCACCATGGAGTCCGAA TCGGAAAGC-3' and antisense, 5'-GGGATCCTTA ACGGTCAGGCCTTT GGAC-3'. The HA-AAMP sequence was amplified from the pcDNA3.1-AAMP plasmid. EGFR gene with FLAG tag was amplified from H1299 cDNA using the primers: sense, 5'-CGGTACCGCCGCCACCATGCGACC CTCCGGGACGGCCGG GGC-3' and antisense, 5'-CCTCGAGTCACTTGT CGTATCGTCTTTGTAGTCTGAAATT CACTGCT-3'.

### 2.5. Western blot assay

Cells were homogenized in lysis buffer on ice for 30 min after

washed with PBS. Samples were centrifuged at 13200 rpm for 15 min followed by protein quantification. Proteins were separated by SDS-PAGE and transferred to polyvinylidene difluoride (PVDF) membranes. Membranes were blocked in 5% nonfat powder in PBST for 1 h at room temperature and then immunoblotted with primary antibodies at 4 °C overnight. After washing with PBS, membranes were incubated with second antibodies conjugated with HRP for 2 h at room temperature. Protein expression was visualized using western blot detection substrate (Millipore, #WBKLS0500).

### 2.6. Construction of stable cell lines

1 μg plasmids containing shRNA sequences (pGIPZ-luc, pGIPZ-shAAMP-1 and pGIPZ-shAAMP-2), 0.25 μg of the envelope plasmid pMD2.G and 0.75 μg of the packaging plasmid psPAX2 were transfected into 293FT cells using Lipofectamine 2000 (Invitrogen). The cell culture media was refreshed 18 h after transfection. Lentivirus supernatant was collected at 48 h and transduced into H1792 cell line for 24 h before cell culture media was refreshed. Monoclonal cells were screened by Puromycin [2 μg/ml] and identified by western blot assay.

### 2.7. High-content microscope analysis

Calu-1 and H1792 cell lines were transfected with 220 nM AAMP siRNAs or 1 μg plasmid pcDNA3.1-AAMP after seeded in 6-well plates. Cells were imaged continuously for 48 h or 60 h using high-content microscope after reseeded in 12-well plates. Cell numbers were counted

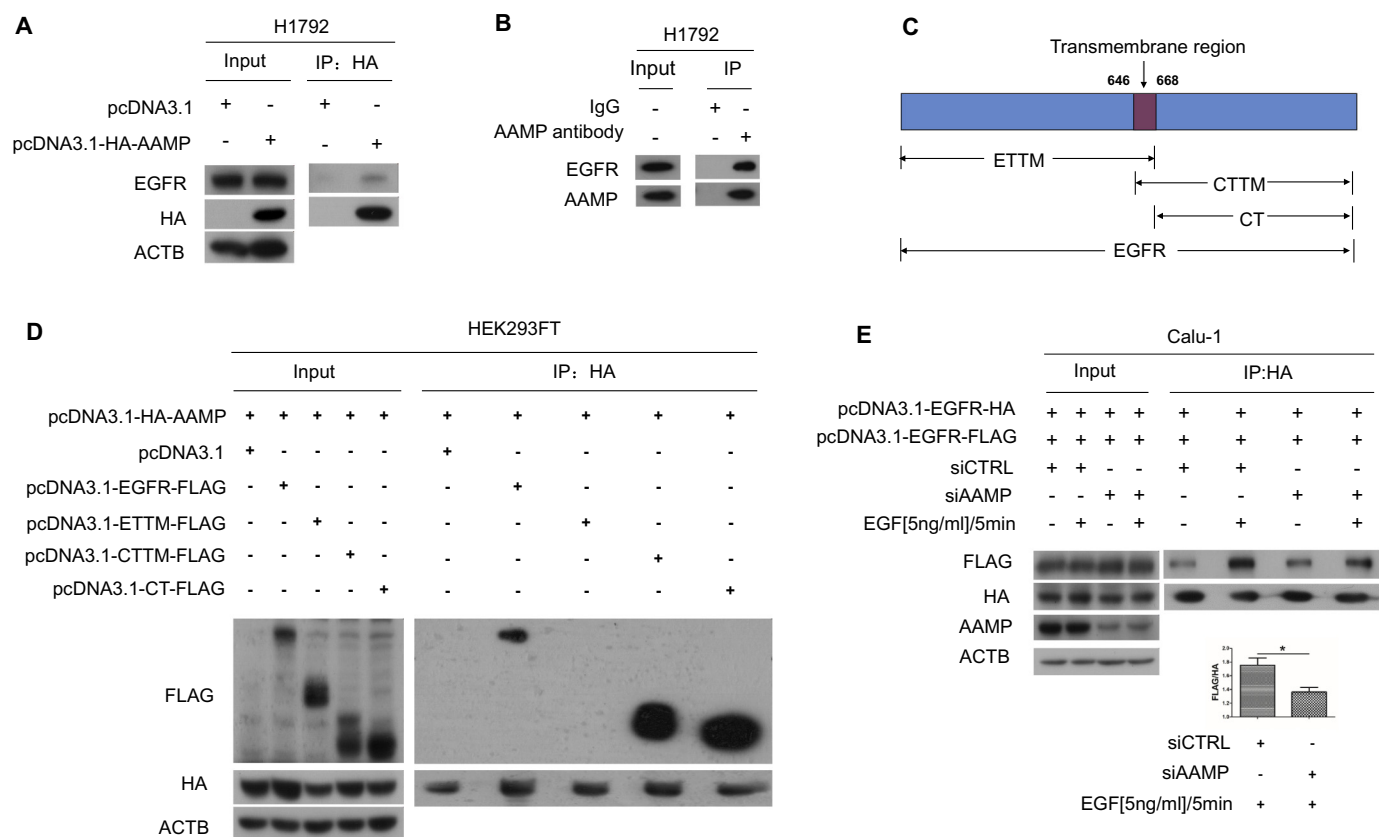


**Fig. 3.** AAMP interacted with EGFR and promoted dimerization. (A) H1792 cells were transfected with pcDNA3.1-HA-AAMP for 24 h then analyzed by co-immunoprecipitation analysis and Western blot. (B) IP and WB analyses of the interaction of endogenous AAMP and EGFR in H1792 cells. (C) EGFR was divided into 3 fragments, including extracellular and transmembrane fragment (ETTM), cytoplasmic and transmembrane fragment (CTTM) and cytoplasmic fragment (CT). (D) The interaction of AAMP with different fragments of EGFR, including CTTM, CT and ETTM was detected by co-immunoprecipitation assay. Western blot was used for FLAG and HA detection. (E) Co-immunoprecipitation assay was performed in Calu-1 cell after transfection with pcDNA3.1-EGFR-FLAG, pcDNA3.1-EGFR-HA, AAMP siRNA and EGF [5 ng/mL]/5 min treatment. HA, FLAG and AAMP were detected by Western Blot. Graphs represent FLAG/HA ratios in EGF treatment groups (means  $\pm$  s.e.m.). The error bars represent the SD, \* $P < .05$ .

at various time points using the high-content microscope software.

## 2.8. SRB assay

H1975 cells transfected with 220 nM AAMP siRNAs for 24 h were reseeded in 96-well plates and then treated with icotinib [20  $\mu$ M] for 0, 24, 48 and 72 h. Cells were fixed using 10% trichloroacetic acid (TCA) for 2 h at 4  $^{\circ}$ C and then washed with sterile water 3 times. Samples were stained with SRB (sulforhodamine B) for 10 min followed by rinse with 1% acetic acid. Absorbance at 450 nm was detected after SRB was dissolved by Tris-base (10 mM, pH = 10). Cell survival rate is positively with 450nm absorbance.

## 2.9. Plate clone assay

Cells were transfected with 220 nM AAMP siRNAs or 1  $\mu$ g AAMP plasmid for 24 h and reseeded in 6 cm dishes at a density of 125 cells/ml. During culture process, culture medium was refreshed every 3 days. Cells were fixed with 10% trichloroacetic acid (TCA) for 2 h at 4  $^{\circ}$ C followed washing with sterile water 3 times. Cell number was calculated after SRB staining without dissolve following above.

## 2.10. Soft agar clone formation assay

The soft agar clone formation assay was performed using 6-well plates. The bottom layer contained 1.5 mL of 0.7% agar in complete medium and the top layer included 1.5 mL of 0.35% agar in complete

medium containing 3000 cells. 200  $\mu$ L fresh medium with 10% (v/v) fetal bovine serum (FBS, Gibco) was added into each hole every 3 days. Cells were cultured for 2–3 weeks. After culturing, the colonies were stained with nitroblue tetrazolium chloride solution (200  $\mu$ L/well), and the number of clones were counted.

## 2.11. EdU assay

H1792 and Calu-1 cells were transfected with 220 nM AAMP siRNAs in 6-well plates for 24 h. The cells were suspended and seeded in 96-well plates at 6000 cells per 100  $\mu$ L, and then cultured for 18 h. Cell proliferation was assessed using an EdU Cell Proliferation ELISA kit (Beyotime Biotechnology, Shanghai, China).

## 2.12. Xenograft study

Female B-NSG 5-week-old mice were purchased from Biocytol (Beijing, China). These mice were divided into 3 groups: H1792/pGIPZ-luc, H1792/pGIPZ-shAAMP-1 and H1792 /pGIPZ-shAAMP-2. A total of  $2 \times 10^6$  cells suspended in 100  $\mu$ L of PBS were injected subcutaneously. The tumor volume was calculated according to the formula  $V = \pi \times (\text{length} \times \text{width}^2)/6$ . All the animal experiments were carried out in accordance with the approval of the Animal Research Committee of Shandong University.

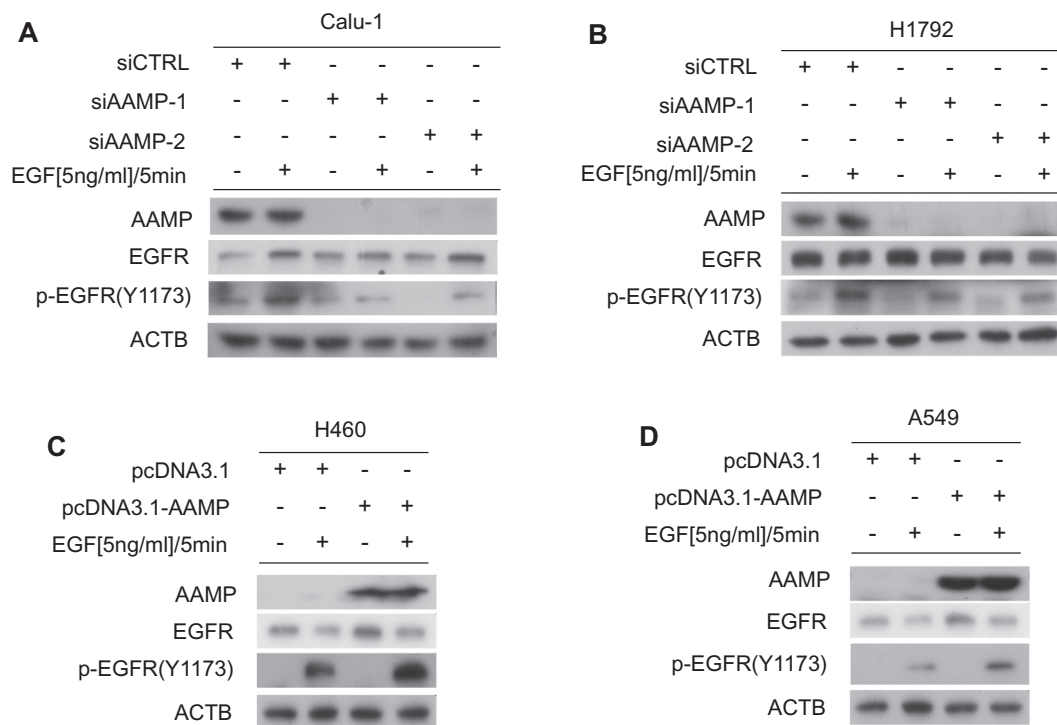


**Fig. 4.** AAMP promoted EGFR phosphorylation at Tyr1173. (A)–(B) AAMP knockdown and EGF [5 ng/mL]/5 min treatment were performed in Calu-1 and H1792 cells. Phosphorylation of EGFR (Y1173) and EGFR were detected by WB. (C)–(D) H460 and A549 cells were transfected with pcDNA3.1-AAMP for 24 h and then treated with EGF [5 ng/mL] for 5 min. The level of phosphorylation EGFR (Y1173) and EGFR were detected by WB. The band of AAMP and ACTB in A549 cells derived from the same membrane of Fig. 5B.

### 2.13. Apoptosis evaluation by flow cytometry

Cells were incubated with annexinV-FITC and PI using an Apoptosis Detection Kit (EnoGene, #BA11100) according to instructions. Flow cytometry was utilized to separate apoptosis cells from normal cells.

### 2.14. Wound-healing scratch assay

Cells were seeded in 6-well plate respectively and cultured overnight. Scratches were made using a p-200 pipette tip when cells were grown to monolayer confluency. Suspended cells were wiped off using PBS washing for 3 times and adherent cells were cultured with optimal medium supplemented with 1% FBS for 48 h–60 h. Images were captured every 12 h. The migration rate was calculated according to images.

### 2.15. Statistical analyses

Image-Pro Plus was used for wound-healing scratch assay. GraphPad Prism 5.0 and Image J were used for statistical analyses. Values are expressed as the mean  $\pm$  standard deviation. Student's *t*-test was used for analysis, and  $P < .05$  was considered significant.

## 3. Results

### 3.1. AAMP promoted cell proliferation and clonogenic ability in NSCLC *in vitro*

Although many reports have studied AAMP in some cancer cells, expression level of AAMP in NSCLC cells has gone undefined. Thus, we measured expression levels of AAMP in several non-small lung cancer cell lines by western blot (Fig. 1A). Results show AAMP was highly expressed in H1792, H157, H1299 and Calu-1; expression was significantly less in H460 and A549 cell lines. Therefore, H1792 and Calu-

1 cell lines were chosen for suppression analysis; H460 and A549 cell lines were selected for overexpression experiments.

We generated two siRNAs, AAMP siRNA #1 and #2, to investigate the function of AAMP in NSCLC cells. Data show cell number was significantly reduced compared with control after AAMP siRNA transfection for 48 h in H460 and Calu-1 cell lines (Fig. S1A). In addition, cell number was significantly less after AAMP knockdown in both Calu-1 and H1792 cells (Fig. 1B and Fig. S1B). In contrast, cellular proliferation rate increased after overexpression of AAMP (Fig. 1C). Consistently, EdU assay results show cell proliferation was significantly less after AAMP knockdown (Fig. 1D and S1C) and increased when AAMP was overexpressed (Fig. S1D).

Using plate clone assays to investigate long-term proliferation of tumor cells, we found the number of tumor clusters decreased after AAMP was silenced in two weeks of culture (Fig. S2A, B and E). As expected, the number of tumor clusters increased after AAMP overexpression (Fig. S2C and D). Meanwhile, we found the ability of proliferation and clonogenicity positively correlated with the level of AAMP (Fig. S3A, B).

We also conducted soft agar clone formation assays *in vitro* to investigate cancer cell growth in a 3D environment in the absence or overexpression of AAMP. We found clone numbers were significantly reduced when AAMP was silenced in Calu-1 cells (Fig. 1E). However, more cell clones were detected after AAMP overexpression compared with the control cells (Fig. 1F). In summary, these data show AAMP promotes NSCLC cell proliferation and clonogenic ability *in vitro*. Interestingly, we observed that the expression level of AAMP was also closely related to cell migration ability (Fig. S3C).

### 3.2. Downregulation of AAMP suppressed H1792 xenograft growth *in vivo*

We explored the role AAMP plays in tumor growth *in vivo*. In these experiments, H1792 pGIPZ-shAAMP-1 and pGIPZ-shAAMP-2 cells, with corresponding control cells pGIPZ-luc, were injected in the subcutis of

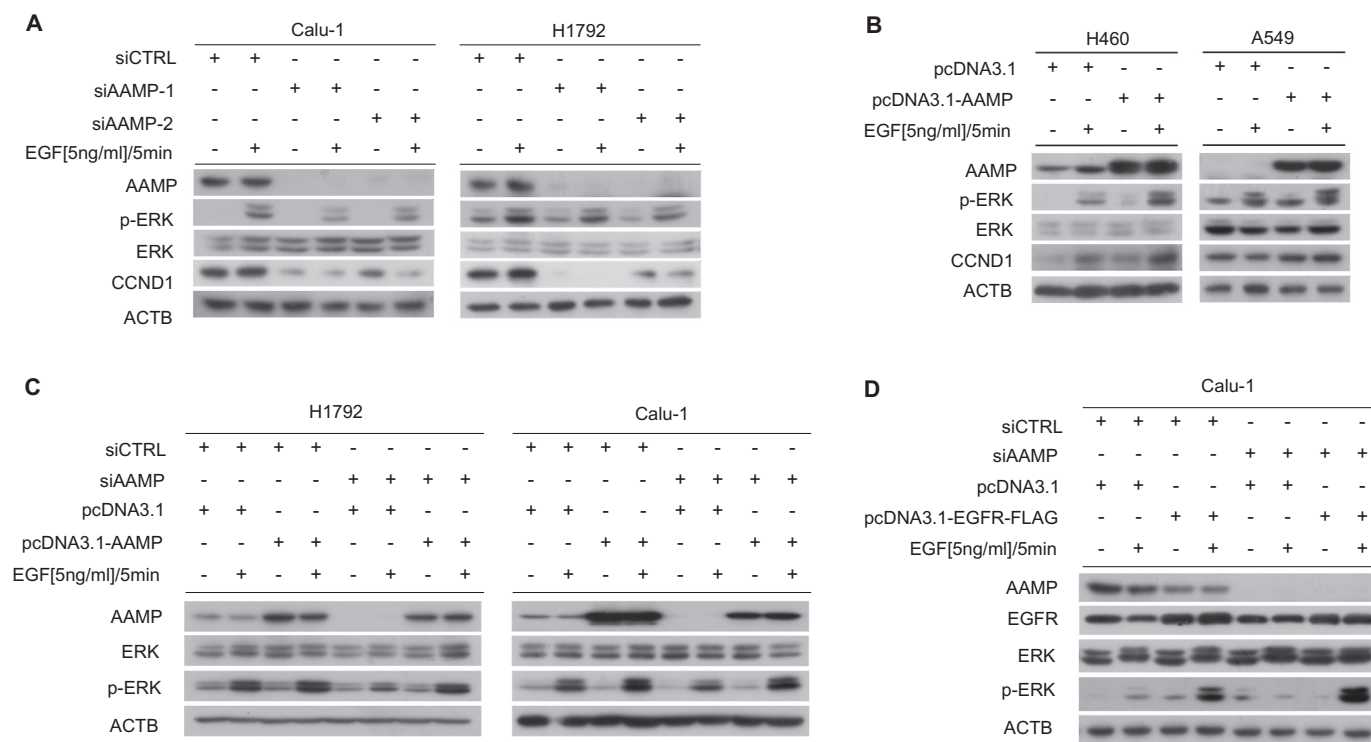


**Fig. 5.** AAMP activated EGFR downstream MAPK signaling pathway. (A) Calu-1 and H1792 cells were transfected with AAMP siRNAs for 24 h and then treated with EGF [5 ng/mL] for 5 min. The level of phosphorylation ERK1/2 (p-ERK1/2), ERK1/2 and CCND1 were detected by Western blot assay. Samples are the same as Fig. 4A and B. (B) H460 and A549 cells were treated with EGF [5 ng/mL] for 5 min after being transfected with pcDNA3.1- AAMP for 24 h. p-ERK1/2, ERK1/2 and CCND1 levels were measured by WB. The sample of A549 is the same as Fig. 4D (C) AAMP was either knocked down or overexpressed in H1792 and Calu-1 cells before EGF [5 ng/mL] treatment for 5 min. ERK1/2 and p-ERK1/2 levels were measured by WB. Graphs represent phospho-ERK1/2/ERK1/2 ratios in EGF treatment groups (means  $\pm$  s.e.m.). The error bars represent the SD, \* $P < .05$ , \*\* $P < .01$  and \*\*\* $P < .001$ . (D) Calu-1 was transfected with AAMP siRNA and pcDNA3.1-EGFR-FLAG. ERK1/2 and p-ERK1/2 levels were evaluated by WB after cells were treated with EGF [5 ng/mL] for 5 min. Graphs represent phospho-ERK1/2/ERK1/2 ratios in EGF treatment groups (means  $\pm$  s.e.m.). The error bars represent the SD, \* $P < .05$  and \*\*\* $P < .001$ .

B-NSG mice. The sizes of heterogeneous tumors were continuously measured until mice were sacrificed. The AAMP levels of the three H1792 cell lines are shown by western blot (Fig. 2A). Both H1792 pGIPZ-shAAMP-1 and pGIPZ-shAAMP-2 cell line xenografts grew more slowly compared with control group (Fig. 2A). In addition, the tumor weights were significantly less in H1792 pGIPZ-shAAMP xenografts compared with the control group (Fig. 2B). Western blot also showed that the phosphorylation of EGFR (Y1173) and ERK were lower in pGIPZ-shAAMP tumor tissues than that in controls (Fig. 2C). No significant difference in mouse weight was found among the three groups (Fig. S1E). These results demonstrate that AAMP promotes tumor cell growth *in vitro* and *in vivo*.

### 3.3. AAMP promoted EGFR dimerization and phosphorylation at Tyr1173

We wanted to understand how AAMP promotes cell proliferation and tumorigenesis and of other proteins participate in this process. Data suggest AAMP and EGFR interact with each other [23]. EGFR belongs to the HER family and plays a critical role in cell growth and proliferation [24]. We performed co-IP experiments to understand the relationship between these two proteins and found AAMP interacts with exogenous and endogenous EGFR in NSCLC cells (Fig. 3A and B). To locate the binding region, we divided EGFR into three fragments, including extracellular and transmembrane fragment (ETTM), cytoplasmic and transmembrane fragment (CTTM) and cytoplasmic fragment (CT) (Fig. 3C). Co-IP results show AAMP interacts with the cytoplasmic part of EGFR (Fig. 3D).

Next, we wonder the biological function of the combination. Given that protein dimerization is a precondition of EGFR activation [25], we asked whether AAMP would promote EGFR dimerization. Here, we

chose EGF as the agonist of EGFR. Calu-1 cells were transfected with the plasmid pcDNA3.1-EGFR-HA and pcDNA3.1-EGFR-FLAG in the presence of AAMP knockdown. Co-IP results show that downregulation of AAMP inhibited EGFR dimerization (Fig. 3E). As reported, phosphorylation of EGFR is crucial for its activity, particularly at the Tyr1173 residue [26,27]. We questioned whether AAMP silencing would repress EGFR phosphorylation. Our experiments show reduction of AAMP inhibited the phosphorylation of EGFR at Tyr1173 (Fig. 4A and B), and increased AAMP led to higher EGFR phosphorylation (Fig. 4C and D). Taken together, our data suggest that AAMP interacts with EGFR and promotes its phosphorylation by facilitating dimerization.

### 3.4. AAMP activated downstream signaling pathway of EGFR

As a receptor tyrosine kinase, EGFR initiates multiple signaling pathways [28]. Among these, the ERK1/2 MAPK pathway induces a wide array of physiological and pathological responses, such as cell growth and proliferation [29,30]. Given that AAMP interacts with EGFR and promotes its phosphorylation, we asked whether AAMP affects ERK1/2, the downstream signaling pathway of EGFR. Our data show ERK1/2 phosphorylation was reduced after AAMP knockdown (Fig. 5A) and increased after AAMP overexpression (Fig. 5B). To test whether the variation of p-ERK1/2 was influenced by AAMP expression, we performed rescue experiments by AAMP inhibition with RNAi in Calu-1 and H1792 cells and expression was recovered by pcDNA3.1-AAMP plasmid transfection. Results show ERK1/2 phosphorylation was restored after AAMP expression was rescued (Fig. 5C).

Considering the significant impact of AAMP on ERK1/2 activation and the interaction between AAMP and EGFR, we wondered if EGFR is an intermediate protein in AAMP-ERK1/2 regulation. We measured

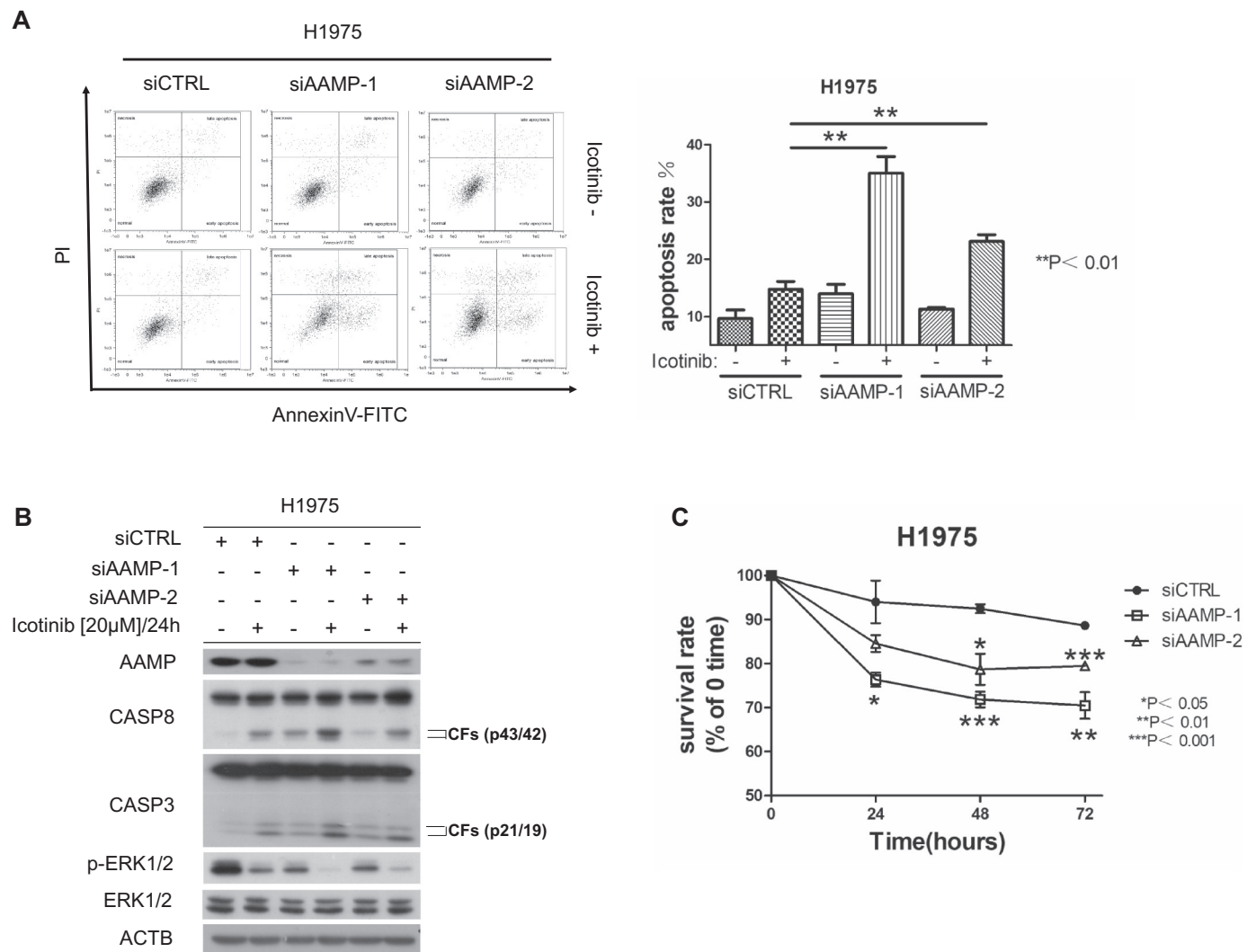


**Fig. 6.** AAMP downregulation elevated the sensitivity to icotinib in H1975 cells. (A) H1975 cells were transfected with AAMP siRNAs for 24 h and then treated with icotinib [20 μM] for 24 h. Flow cytometry was used to measure apoptosis rate ( $n = 4$ ). (B) H1975 cells were treated with icotinib [20 μM] for 24 h after being transfected with AAMP siRNAs for 24 h. The cleavage of caspase 8 and caspase 3 was detected by Western blot. (C) H1975 cells were reseeded in 96-well plate after AAMP downregulating. Cells were fixed separately after icotinib [20 μM] treated for 0, 24, 48 and 72 h. SRB assay was performed to detect survival rate ( $n = 5$ ).

phosphorylation level of ERK1/2 after AAMP knockdown and EGFR overexpression in the same cells. Western blot data show ERK1/2 phosphorylation was repressed after AAMP silencing. Interestingly, EGFR overexpression recovered p-ERK1/2 level after AAMP silencing (Fig. 5D). These data demonstrate EGFR overexpression rescues the reduction of ERK1/2 phosphorylation caused by AAMP inhibition, indicating AAMP activates ERK1/2 through EGFR activation.

### 3.5. AAMP silencing elevated sensitivity to icotinib in H1975 cells

H1975 cells were confirmed as a first-generation EGFR-TKIs resistance cell lines with two EGFR activating mutations (L858R and T790M). Thus, we wonder whether AAMP suppression elevates sensitivity to icotinib in H1975 cells. AAMP siRNA transfection was performed in H1975 cells for 24 h. Apoptosis was detected by western blot and flow cytometry after icotinib treatment at 20 μM for 24 h. Results show that combination between AAMP inhibition and icotinib increased the percentage of apoptosis cells (Fig. 6A) and cleaved forms of caspase-8 and caspase-3 (Fig. 6B). Furthermore, the percentage of survival cells was decreased in a time-dependent manner with icotinib [20 μM]/24 h treatment when AAMP was silenced (Fig. 6C). These data suggest AAMP downregulation enhanced sensitivity to icotinib in H1975 cells

with TKIs resistance EGFR mutations.

### 3.6. EGFR has minimum influence on AAMP expression

Since AAMP plays an important role in EGFR activation, we wonder whether EGFR exert an influence on AAMP. As AAMP is an adaptor protein, and no enzymatic activity has been found yet. Thus, we detected the level of AAMP after EGFR knockdown in EGFR wild type and mutant cell lines respectively. The results showed that EGFR repression had minimum effect on AAMP expression (Fig. S4A and B). In addition, we transfected EGFR single mutation (L858R) and double mutation (L858R/T790M) plasmids into NSCLC cells to test the protein level of AAMP. Similarly, no big difference in AAMP levels was found (Fig. S4C). These results indicate AAMP regulates EGFR activity, while EGFR has minimum effect on AAMP level.

### 3.7. AAMP inhibition promoted apoptosis caused by doxorubicin in NSCLC

Our previous studies have found that doxorubicin induces EGFR downregulation in dose-dependent and time-dependent manners in NSCLC cells (Fig. 7A). Besides, evidence above revealed that suppression of AAMP impaired proliferation and survival through EGFR

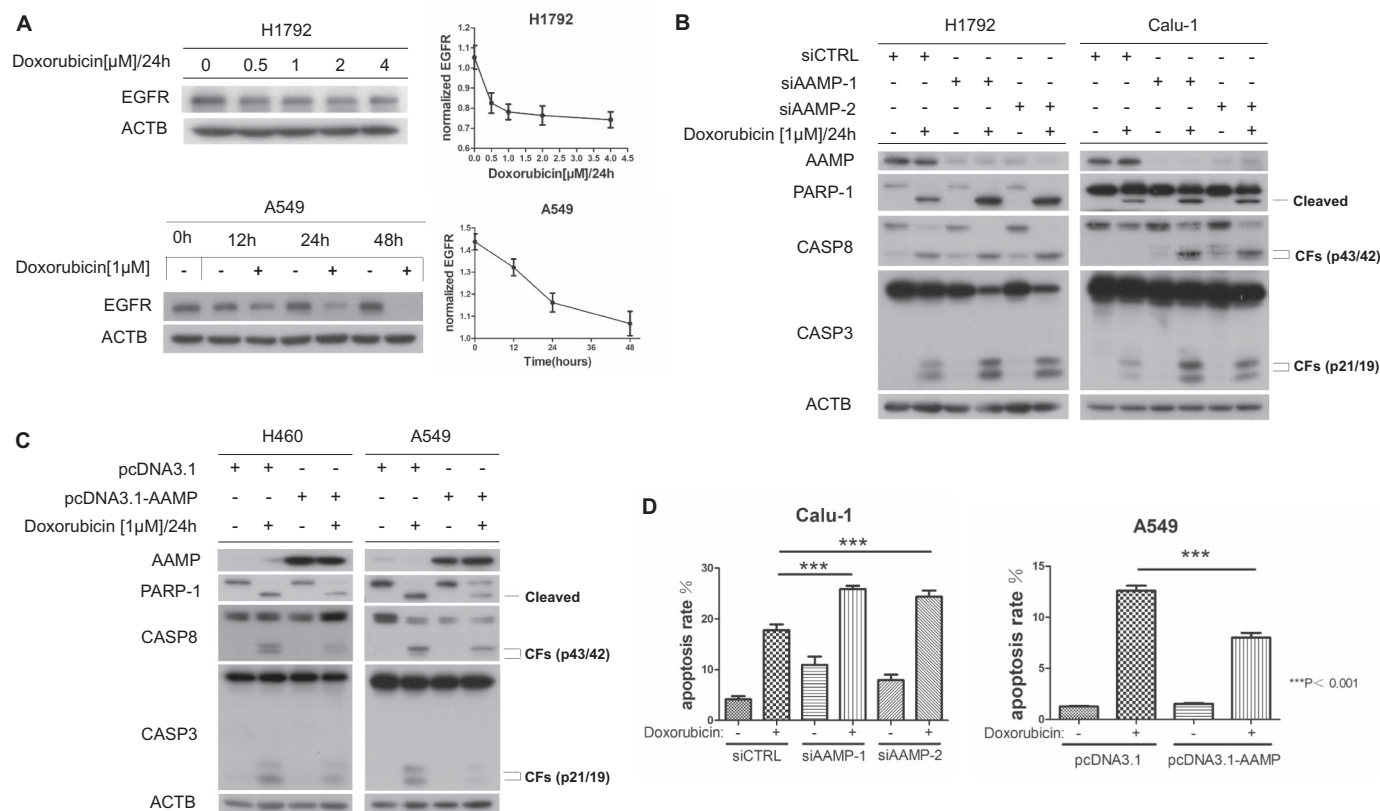


**Fig. 7.** AAMP reduced the sensitivity to doxorubicin in NSCLC cells. (A) H1792 cells were treated with doxorubicin at 0, 0.5, 1, 2, 4  $\mu$ M for 24 h. A549 cells were treated with doxorubicin at 1  $\mu$ M for 0, 12, 24 and 48 h. The level of EGFR was measured by WB. (B) AAMP downregulation and doxorubicin [1  $\mu$ M]/24 h treatment were performed in H1792 and Calu-1 cells. WB was used to detect the cleavage of caspase 8 and caspase 3. (C) H460 and A549 cells were treated with doxorubicin [1  $\mu$ M] for 24 h after being transfected with pcDNA3.1-AAMP. The cleavage of caspase 8 and caspase 3 were measured by WB. (D) AAMP downregulation and upregulation were performed in Calu-1 and A549 cells. Apoptosis rate was detected by flow cytometry after doxorubicin [1  $\mu$ M]/24 h treatment (n = 4).

activation inhibiting in NSCLC. To test the specific role of AAMP in apoptosis caused by doxorubicin in cancer cells, we treated H1792 and Calu-1 cells with doxorubicin for 24 h after AAMP siRNA transfection. The data show that AAMP downregulation enhanced cleavage of caspase-8 and caspase-3 caused by doxorubicin significantly (Fig. 7B), while the cleavage in H460 and A549 cells overexpressing AAMP was declined (Fig. 7C). We achieved similar results using flow cytometry (Fig. 7D). These results collectively demonstrate that the combination of doxorubicin with AAMP inhibition potently induces apoptosis in NSCLC cells.

#### 4. Discussion

AAMP is found in many tumors which suggests it plays important role in cancers [6–8]. AAMP contains a repeated-WD40 domain that is correlated with functions such as apoptosis, autophagy, motility and growth. Therefore, it could be a multifunctional protein. However, nowadays we just have realized a little bit about it, such as inhibiting NF- $\kappa$ B signaling pathway [6] and promoting angiogenesis [31]. Its molecular mechanism in cancer cells remains largely unclear. In our study, we found that AAMP suppression inhibited proliferation *in vitro* in NSCLC cells. Moreover, heterogeneous tumors grow more slowly at the condition of AAMP silence in a xenograft mouse model. These data remind the importance of AAMP in tumorigenesis. Indeed, AAMP is a novel marker of lung cancer progression [13,14]. Because of its unique sequence, AAMP is likely to function through the interaction with other proteins. Accidentally, proteomic analysis showed that AAMP interacts with EGFR [23], which provides clues for mechanism research.

There are > 58 encode transmembrane protein receptor tyrosine kinases (RTKs) in cells. Among them, epidermal growth factor receptor

(EGFR) was the first one identified and linked to cancer. Thus, it is the most intensively studied RTK all over the world. However, the mechanism of EGFR activation is still not fully understood. EGFR functions as an oncogenic protein and is correlated with cell growth, differentiation and motility [16]. It exists as two forms, monomers and dimers. When transformed from monomer state into dimer, EGFR is activated and autophosphorylated at tyrosine 1173, 1068 and 1086 sites to trigger downstream signal pathways, such as RAS-RAF-MEK-ERK, PI3K-AKT and PLC $\gamma$  [32], which eventually promotes cell survival, proliferation and anti-apoptosis. In NSCLC cells, EGFR overexpression and continuous activation are widespread and provide momentum in tumorigenesis [33]. Meanwhile, tumor cells may benefit from dysregulation of EGFR to obtain drug resistance. Thus, how to block activation of EGFR effectively is critical for NSCLC therapy. Nowadays, most studies of EGFR overactivity focus on its own mutations and overexpression and researches about accessory protein are rarely found.

Here, we reported AAMP protein contributing to EGFR activation. We noted that AAMP silencing inhibited EGFR phosphorylation at tyrosine1173 site, which reminded us the important role of AAMP in EGFR activation. Co-IP experiments showed that AAMP interacted with EGFR and less dimers of EGFR were detected when AAMP was down-regulated. These results demonstrated that AAMP may be a helper in the process of dimerization to promote EGFR phosphorylation and activate downstream signaling pathways in NSCLC cells. Subsequent data revealed that AAMP inhibition suppressed phosphorylation of ERK1/2 and proliferation as expected.

Oncogene-targeted therapy has always been favored and achieves better effects. Administration of EGFR tyrosine kinase inhibitors (TKIs) is widely used in NSCLC treatment with a higher overall response rate, longer overall survival and lower incidence of adverse reactions relative

to drug chemotherapy [34,35]. Unfortunately, almost all patients develop acquired resistance after EGFR TKI treatment for 1 year. Thus, combination is a better choice than EGFR TKI therapy alone. Currently, multiple combination treatments have developed, such as association of PD1 blockade with EGFR TKIs [36], Erlotinib plus Cabozantinib [37] and combination of EGFR TKIs with radiotherapy [38]. In our study, we found AAMP suppression elevated sensitivity to icotinib, the first generation EGFR TKI, in drug-resistant H1975 cells. This means AAMP can both promote EGFR activation and improve its resistance to TKI. Furthermore, our results also showed that AAMP downregulation could improve apoptosis caused by doxorubicin in NSCLC cells. Those suggest that AAMP may play an important role in drug-resistance include EGFR TKI and chemotherapeutics. Therefore, it is significant to develop inhibitors of AAMP or drugs downregulate it and combination of them with EGFR TKI or chemotherapy drugs may achieve extraordinary effects.

Taken together, our data demonstrate that loss of AAMP inhibits cell proliferation by impairing EGFR activation and enhances icotinib and doxorubicin sensitivity in EGFR mutation and wide-type NSCLC cells. In this study, we identified a regulator of EGFR dimerization and highlighted a novel mechanism of EGFR regulation in NSCLC cells, suggesting that approaches to downregulate AAMP or interrupt the interaction of AAMP and EGFR can enhance the efficacy of EGFR-targeted therapy in cancer treatment. Meanwhile, the downregulation of AAMP can also enhance the lethal effect of chemotherapy drugs. These findings may offer key insights into developing novel strategy to treat lung cancers.

Supplementary data to this article can be found online at <https://doi.org/10.1016/j.cellsig.2019.05.004>.

## Acknowledgement

Special thanks to Dr. Austin Cape for his helpful editing advances.

## Funding

This work was supported by the grants from National Natural Science Foundation of China (81672855, 31571422 and 31771526) and Shandong Provincial Key Laboratory of Animal Cell and Developmental Biology (SPKLACDB-2019017 and SPKLACDB-2019012).

## Ethics approval

Not applicable.

## Competing interests

The authors declare that they have no competing interests.

## Authors' contributions

Ling Su and Xiangguo Liu conceived the project. Shun Yao, Xiangguo Liu, and Ling Su designed experiments and analyzed data and drafted the manuscript. Shun Yao, Feifei Shi and Wenbo Sun and Yifeng Zhang conducted the experiments. Xiaoyang Sun, Yingying Wang and Xianfang Liu contributed to animal experiments. All authors have read and approved the final manuscript.

## References

- [1] M.E. Beckner, H.C. Krutzsch, M.L. Stracke, S.T. Williams, J.A. Gallardo, L.A. Liotta, Identification of a new immunoglobulin superfamily protein expressed in blood vessels with a heparinbinding consensus sequence, *Cancer Res.* 55 (1995) 2140–2149.
- [2] L. Yu, C. Gaitatzes, E. Neer, T.F. Smith, Thirty-plus functional families from a single motif, *Protein Sci.* 9 (2000) 2470–2476.
- [3] Z. Caiguo, Z. Fan, The multifunctions of WD40 proteins in genome integrity and cell cycle progression, *J. Genomics* 3 (2015) 40–50.
- [4] M.E. Beckner, H.C. Krutzsch, S. Klipstein, S.T. Williams, J.E. Maguire, et al., AAMP, a newly identified protein, shares a common epitope with alpha-actinin and a fast skeletal muscle fiber protein, *Exp. Cell Res.* 225 (1996) 306–314.
- [5] M.E. Beckner, L.A. Liotta, AAMP, a conserved protein with immunoglobulin and WD40 domains, regulates endothelial tube formation *in vitro*, *Lab. Investig.* 75 (1996) 97–107.
- [6] H. Bielig, B. Zurek, A. Kutsch, M. Menning, D.J. Philpott, P.J. Sansonetti, et al., A function for AAMP i-n Nod2-mediated NF- $\kappa$ B activation, *Mol. Immunol.* 46 (2009) 2647–2654.
- [7] Reid H. M, Wikström K, Kavanagh D. J, Mulvaney E. P, Kinsella B. T. Interaction of angio-associated migratory cell protein with the TP $\alpha$   $\pm$  and TP $\beta$  isoforms of the human throbboxane A2, receptor. *Cell. Signal* 2011; 23: 700–717.
- [8] Y. Yin, A.J. Sanders, W.G. Jiang, The impact of angio-associated migratory cell protein (AAMP) on breast cancer cells *in vitro* and its clinical significance, *Anticancer Res.* 33 (2013) 1499–1509.
- [9] P. Holvoet, P. Sinnave, Angio-associated migratory cell protein and smooth muscle cell migration in development of restenosis and atherosclerosis, *J. Am. College Cardiol* 52 (4) (2008) 312–314.
- [10] F. Vogt, A. Zerneck, M. Beckner, N. Krott, A.K. Bosserhoff, R. Hoffmann, et al., Blockade of angio-associated migratory cell protein inhibits smooth muscle cell migration and neointima formation in accelerated atherosclerosis, *J. Am. Coll. Cardiol.* 52 (2008) 302–311.
- [11] H. Jianjun, Q. Juhui, Z. Yimin, Z. Tao, Y. Tieying, X. Xiang, et al., AAMP regulates endothelial cell migration and angiogenesis through RhoA/Rho kinase signaling, *Ann. Biomed. Eng.* 44 (3) (2015) 830–832.
- [12] Y. Yukun, J.S. Andrew, F. Li, G.J. Wen, Knockdown of AAMP impacts on HECV cell functions *in vitro* and affects the expression of VE-cadherin, *Agiology* 2 (2014) 2.
- [13] S.V. Allander, N.N. Nupponen, M. Ringner, G. Hostetter, G.W. Maher, N. Goldberger, et al., Gastrointestinal stromal tumors with *KIT* mutations exhibit a remarkably homogeneous gene expression profile, *Cancer Res.* 61 (2001) 8624–8628.
- [14] A. Adeyinka, E. Emberley, Y. Niu, L. Snell, L.C. Murphy, H. Sowter, et al., Analysis of gene expression in ductal carcinoma *in situ* of the breast, *Clin. Cancer Res.* 8 (2002) 3788–3795.
- [15] Y. Yarden, M. Sliwkowski, Untangling the ErbB signaling network, *Nat. Rev. Mol. Cell Bi-ol* 2 (2001) 127–137.
- [16] J. Schlessinger, Ligand-induced, receptor-mediated dimerization and activation of EGF re-ceptor, *Cell* 110 (2002) 669–672.
- [17] S. Maurizio, B. Jose, The epidermal growth factor receptor pathway: a model for tar-geted therapy, *Mol. Pathways* 12 (18) (2006).
- [18] F.R. Hirsch, G.V. Scagliotti, C.J. Langer, M. Varella-Garcia, W.A. Franklin, Epidermal growth factor family of receptors in preneoplasia and lung cancer: per-spectives for targeted therapies, *Lung Cancer* 41 (Suppl. 1) (2003) S29–S42.
- [19] M.S. Giulia, L.S. Maurizio, I. Simona, C. Francesca, S. Roberta, Z. Michele, et al., Targeting EGFR in non-small-cell lung cancer: lessons, experiences, strategies, *Respir. Med.* 106 (2012) 173–183.
- [20] K. Sirichat, W.J. Seung, S.K. Chang, M. Dong, H. ShinYoon-Hwae, K. Kyujung, et al., Increased EGFR expression induced by a novel oncogene, CUG2, confers resistance to doxorubicin through Stat1-HDAC4 signaling, *Cell. Oncol.* 40 (2017) 549–561.
- [21] A. Tartarone, R. Lerosé, Clinical approaches to treat patients with non-small cell lung cancer and epidermal growth factor receptor tyrosine kinase inhibitor acquired resistance, *Ther. Adv. Resp. Dis* 9 (2015) 242–250.
- [22] J. Remon, T. Moran, M. Majem, N. Reguart, E. Dalmau, D. Marquez-Medina, et al., Acquired resistance to epidermal growth factor receptor tyrosine kinase inhibitors in EGFR-mutant non-small cell lung cancer: a new era begins, *Cancer Treat. Rev.* 40 (2014) 93–101.
- [23] J. Tong, P. Taylor, M.F. Moran, Proteomic analysis of the epidermal growth factor receptor (EGFR) interactome and post-translational modifications associated with receptor endocytosis in response to EGF and stress, *Mol. Cell. Proteomics* 13 (7) (2014) 1644–1658.
- [24] M.A. Lemmon, J. Schlessinger, Cell signaling by receptor tyrosine kinases, *Cell* 141 (2010) 1117–1134.
- [25] K. Ferguson, M. Berger, J. Mendrola, H. Cho, D. Leahy, M. Lemmon, EGF activates its receptor by removing interactions that autoinhibit ectodomain dimerization, *Mol. Cell* 11 (2003) 507–517.
- [26] N. Bessman, A. Bagchi, K.M. Ferguson, M. Lemmon, Complex relationship between ligand binding and dimerization in the epidermal growth factor receptor, *Cell Rep.* 9 (2014) 1306–1317.
- [27] Y. Okabayashi, Y. Kido, T. Okutani, Y. Sugimoto, K. Sakaguchi, M. Kasuga, Tyrosines 1148 and 1173 of activated human epidermal growth factor receptors are binding sites of Shc in intact cells, *J. Biol. Chem.* 269 (1994) 18674–18678.
- [28] W. Ping, W. Zhixiang, Epidermal growth factor receptor cell proliferation signaling pathways, *Cancers* 9 (2017) 52.
- [29] D.K. Morrison, MAP kinase pathways, *Cold Spring Harb. Perspect. Biol.* 4 (2012) a011254.
- [30] T. Lewis, P. Shapiro, N. Ahn, Signal transduction through MAP kinase cascades, *Adv. Cancer Res.* 74 (1998) 49–139.
- [31] E.B. Marie, J. Syamala, A.P. Virginia, Extracellular angio-associated migratory cell protein plays a positive role in angiogenesis and is regulated by astrocytes in co-culture, *Microvasc. Res.* 63 (2002) 259–269.
- [32] A.K. Jed, P.F. Michael, L. Zujun, Recent advances of novel targeted therapy in non-small cell lung cancer, *J. Hematol. Oncol.* 2 (2009) 2.
- [33] D. Bhagirathbhai, H. William, S. Amanda, L. Yanyan, Emerging therapeutic agents for lung cancer, *J. Hematol. Oncol.* 9 (2016) 138.

- [34] T. Mitsudomi, S. Morita, Y. Yatabe, et al., West Japan Oncology Group Gefitinib versus cisplatin plus docetaxel in patients with non-small-cell lung cancer harbouring mutations of the epidermal growth factor receptor (WJTOG3405): an open label, randomised phase 3 trial, *Lancet Oncol* 11 (2) (2010) 121–128.
- [35] C. Zhou, Y.L. Wu, G. Chen, et al., Erlotinib versus chemotherapy as first-line treatment for patients with advanced EGFR mutation-positive non-small-cell lung cancer (optimal, CTONG-0802): a multicentre, open-label, randomised, phase 3 study, *Lancet Oncol* 12 (8) (2011) 735–742.
- [36] Myung-Ju Ahn, Jong-Mu Sun, Se-Hoon Lee, Jin Seok Ahn, Keunchil Park, EGFR TKI combination with immunotherapy in non-small cell lung cancer, *Expert Opin. Drug Saf.* 16 (4) (2017) 465–469.
- [37] K.L. Reckamp, P.H. Frankel, N. Ruel, P.C. Mack, B.J. Gitlitz, T. Li, et al., Phase II trial of cabozantinib plus erlotinib in patients with advanced epidermal growth factor receptor (EGFR)-mutant non-small cell lung cancer with progressive disease on epidermal growth factor receptor tyrosine kinase inhibitor therapy: a California Cancer Consortium phase II trial (NCI 9303), *Front. Oncol.* 9 (2019) 132.
- [38] Z.Y. He, M.F. Li, J.H. Lin, D. Lin, R.J. Lin, Comparing the efficacy of concurrent EGFR-TKI and whole-brain radiotherapy vs EGFR-TKI alone as a first-line therapy for advanced EGFR-mutated non-small-cell lung cancer with brain metastases: a retrospective cohort study, *Cancer Manag. Res.* 11 (2019) 2129–2138.